TIME-DEPENDENT FREIGHT ORIGIN-DESTINATION SYNTHESIS

Iván Sánchez-Díaz, Rensselaer Polytechnic Institute, Troy, New York, 12180, sanchi2@rpi.edu

José Holguín-Veras, Rensselaer Polytechnic Institute, Troy, New York, 12180, jhv@rpi.edu

Jeff Ban, Rensselaer Polytechnic Institute, Troy, New York, 12180, banx@rpi.edu

ABSTRACT

This paper proposes a novel approach to model aggregated freight demand in urban environments. The analytical models proposed improve current techniques by incorporating the time-dependent tour-based behavior of freight vehicles. Furthermore, an origin destination synthesis model is proposed to overcome the need of expensive surveys to assess freight demand patterns by incorporating data from secondary sources. Two sets of formulations are proposed, the first one is the time-dependent entropy maximization (TD-EM) problem that takes advantage of TD freight trip generation, while the second one is a time-dependent origin destination synthesis (TD-ODS) that incorporates TD traffic counts to produce an OD matrix. These formulations are tested using a simplified experimental setup. TD-EM model obtains the best performance, followed by the TD-ODS and the Static-EM models.

Keywords: demand modeling, time-dependence, urban freight tours, origin-destination synthesis

1. INTRODUCTION

Urban transportation systems are basic components of cities' social, economic and physical structure. The design and planning of these systems have been traditionally aimed at improving mobility, modifying growth patterns and enhancing economic development; though in more recent years they have been redirected to also serve other national and community objectives (e.g., social equity, sustainability) (Meyer and Miller, 1984). To make this possible, urban planners count on a number of tools to anticipate the consequences of alternative actions. In particular, transportation demand models play an important role to support planning by providing a simplified representation of a real world problem. In the classic transport model, the starting point is to consider a zoning and network system, and the collection of planning, calibration and validation data. The data is used to estimate the total number of trips produced and attracted by each zone; these trips are then allocated to particular destinations under the form of an OD matrix. Next steps include the mode choice for the trips and the corresponding traffic assignment (Ortúzar and Willumsen, 2001). In the case of freight, the complexity of interacting decision makers, the availability of suitable data, and the data processing requirements (among others), represent a threat for applying the classical modeling approach. These issues faced by freight transportation systems have unveiled the necessity of new freight urban demand models.

In practice, paradigms used in passenger transportation have been adapted to estimate freight related trips. However this correspondence is problematic; one of the reasons is that freight demand has different dimensions: it can be calculated in trips (loaded and empties), commodities or value. Therefore, two major interrelated modeling platforms are often used: commodity based models and trip based models. This distinction is important because while commodity flows are the consequence of an economic interaction between two entities or zones, transportation of goods is a derived demand that might not follow the same geographical pattern (Ogden, 1978). Freight models can incorporate this consideration by studying tour-based behavior.

Given the complexity of tour behavior, researchers have proposed a number of techniques to model freight tours. These formulations can be roughly classified into simulation, hybrid, and analytical models. Among the simulation models, one could list Boerkamps and van Binsbergen (1999), Liedtke and Schepperle (2004), Stefan et al. (2005), Liedtke (2006), Hunt and Stefan (2007), Routhier and Toilier (2007), and Liedtke (2009). Stefan et al. (2005) and Hunt and Stefan (2007) propose an agent-based microsimulation to model commercial vehicles in Calgary, Canada. In their model, tours are constructed using a “rubber-banding” approach, and a fleet-allocator simulation model. Routhier and Toilier (2007) develop a simulation model (FRETURB) to reproduce tour patterns observed on an area of study. These patterns are obtained from a large scale urban freight survey that is regularly conducted in France. Their model has been successfully applied to a number of French cities. Boerkamps and van Binsbergen (1999) develop the GoodTrip to study urban freight distribution in Groningen, The Netherlands. The GoodTrip model estimates commodity flows according to the spatial distribution of activities, and convert these flows to vehicle tours using micro-simulations based on the origin’s activity type. Liedtke and Schepperle (2004) and Liedtke (2009) propose an actor-based approach to model freight movements. The model proposed (InterLOG) generates tour-based truck trips based on estimated commodity flows between companies and a market simulation module. Although the model was originally designed for intercity freight trips, its structure may be amenable for urban freight tours.

However, although simulation models have proven very useful to describe existing conditions, an added analytical component provides a robust foundation for modeling purposes, particularly, if the analytical component is supported by proper behavioral and/or economic axioms (Holguín Veras et al., 2012). Formulations that combine analytical models and simulations are hybrids. There is a significant number of them (Taniguchi and Thompson, 2002; van Duin et al., 2007; Wisetjindawat et al., 2007; Donnelly, 2010). For instance, Taniguchi and Thompson (2002) propose a model that consists of a vehicle routing problem and a dynamic traffic simulation, where the demand for each carrier is randomly simulated. Wisetjindawat et al. (2007) use a commodity-based model to estimate production, consumption, and distribution in Tokyo, and then convert the commodity flows into vehicle flows using a fleet allocator simulation, and subsequent vehicle routing simulations. van Duin et al. (2007) studies auctions in the spot market, and they affect tours structure. A simulation model assigns the loads from the spot market to each carrier, and thereby determines which tours are taking place. Donnelly (2007) uses a simulation model to fuse data from different sources and obtain aggregate commodity flows. Deliveries are then consolidated using a shipment assignment module based on Monte Carlo simulations and a vehicle routing algorithm.

Other models determine freight tours using analytical procedures based on behavioral, economic or statistical axioms. For instance, Holguín-Veras (2000), Thorson (2005), and Xu and Holguín-Veras (2008) use economic principles to find the commodity and freight-vehicle flows that meet freight market equilibrium conditions. These models use a bi-level formulation that relates the suppliers' decisions (e.g., production level, delivery routes and profit margin) to a market competition environment. Given the combinatorial nature of these formulations, solving them is computationally challenging, and only small instances can be solved at optimality using state-of-the-art algorithms. Thorson (2005), and Xu and Holguín-Veras (2008) assess the performance of their models with satisfactory results for mid-size problems. A general formulation for this family of models is presented in Holguín-Veras et al. (2012) and consists of a spatial price equilibrium model that computes the corresponding commodity flows and vehicle-trips for the case integrated shipper-carrier operations. This formulation is successfully solved with the assistance of heuristic procedures.

As shown in the previous review, in order to develop efficient transportation models, planning agencies need extensive datasets. These data requirements are in general very expensive and simulations that do not use a significant amount of data as input are simply not useful for planning and decision-making processes. Therefore, few metropolitan planning organizations use exclusive models for freight. Yet, new models use traffic counts to bypass the need of expensive OD flows surveys and open the option to introduce time-dependent effects. This paper proposes an enhanced freight trip distribution model and a freight origin-destination synthesis model. These analytical models improve current techniques by including the time-dependent (TD) tour-based behavior of freight vehicles and incorporating data from secondary sources (e.g., traffic counts).

This document is comprised of three sections in addition to this introduction. Section 2 presents the research approach and basic definitions. Section 3 discusses the results from the experiments and Section 4 presents the conclusions from this research.

2. THEORETICAL BACKGROUND AND RESEARCH APPROACH

This chapter presents the overall approach of the models proposed and some basic definitions including notation. Figure 1 presents the general structure, and the different components of the model.

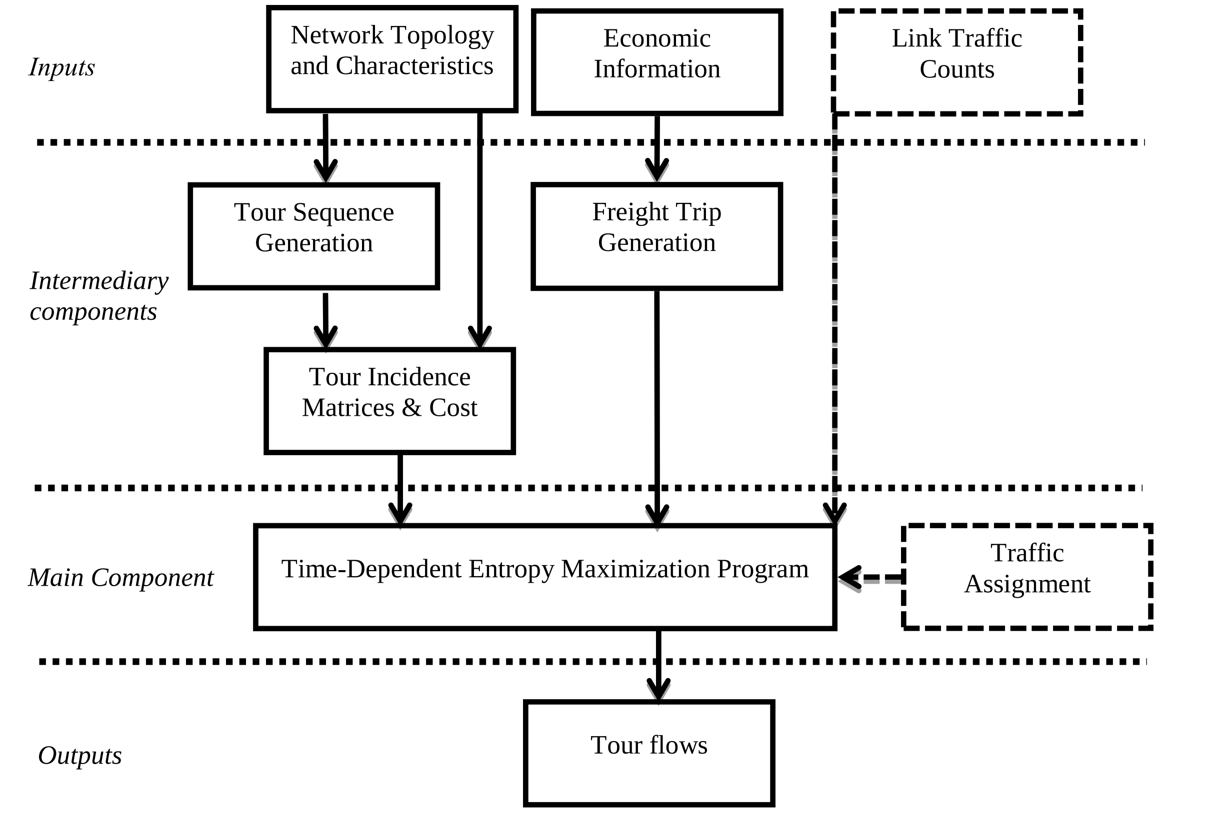

Note: Link traffic counts and traffic assignment modules are used in the time-dependent ODS, but not in the regular time-dependent tour-based formulation

Figure 1: Model Components

As shown, the main inputs are the network topology and characteristics, the zonal economic data (used to estimate freight trip generation), and traffic volumes on links. The first step is the process of tour sequence generation that creates the set of input tours used by the TD-EM and TD-ODS models. These tour sequences can be obtained directly from GPS data or can be estimated using discrete choice models, see (Wang and Holguín-Veras, 2008).

Using the output from the tour sequence generation, a second process produces the tour-centroid incidence matrix that indicates which TAZs are visited by each tour, and the cumulative cost vector for each tour. These vectors are highly dependent on the links travel time and the handling time at each zone; these impedance measures may vary according to the time of the day. The resulting incidence matrix is crucial because it defines the time interval within which a tour reaches each centroid, and therefore determines which combinations of tours meet time-dependent demand constraints. These demand constraints are determined using the third component, which provides freight trip generation for each TAZ and each time interval. The main component is the TD-EM model that finds the most likely meso states (tour flows), given the demands and cost constraints, using the results from the previous components as inputs. In the case of ODS, a traffic assignment module is included to obtain link traffic volumes estimates and compare them to the counts. This traffic assignment module may use an all or nothing algorithm or a multi-path algorithm (for each interval) to estimate the proportion $\bar{p}_m^{ka}$ of flow assigned to each link studied. The outputs from the overall model are tour flows that could be translated if desired into an OD matrix.

2.1. Basic Definitions

It is important to start by explaining the distinction between the interrelated concepts of *tour sequence* and *tour flows*. A tour sequence is an ordered listing of the nodes that are visited as part of a generic tour *m*: $S_m=[n_1,n_2,\ldots,n_m]$; while the tour flow x_m represents the number of vehicles that traverse the node sequence that defines the tour *m*. This distinction is important because, since this is an aggregate model that focuses on depicting travel to/from transportation analysis zones (TAZs), it is very likely that numerous vehicles follow the same sequence, as the nodes are defined in terms of geographic areas (the TAZs) containing significant numbers of commercial establishments.

Studying the evolution of freight vehicle traffic over the day provides invaluable insight for travel demand management strategies and the assessment of urban freight policies. To this effect, the model considers the time-dependent effects on: (1) tour starting time; and (2) arrival/departure to/from each TAZ. The time domain is discretized in Δ intervals, and the tour's starting time is handled by replicating each tour Δ times; while the arrival/departure times to/from centroids are estimated using the tour sequences, the topology of the network, and the average travel and handling times. For each tour *m* a binary variable g_{im}^k indicates if the tour reaches TAZ *i* during the interval *k,* as shown in the following equation:

$$g_{im}^k = \begin{cases} 1, \; if \;\; (k-1)\Delta \le (d-1)*\Delta + \eta_m^i(d) < k\Delta \\ 0, \text{ otherwise} \end{cases} \tag{1}$$

Where:

$\eta_m^i(d)$:The elapsed total time of tour m that started at interval d when it arrives to TAZ i (this includes handling time in the previously visited centroids).

A similar procedure is followed to mark the time interval where the tours leave the TAZs. The only difference is that the elapsed time includes the handling times at all the preceding TAZs (except the base). The corresponding binary variable is γ_{im}^k , is:

$$\gamma_{im}^k = \begin{cases} 1, \; if \;\; (k-1)\Delta \le (d-1)*\Delta + \eta_m^i(d) + h_i < k\Delta \\ \quad 0, \text{ otherwise} \end{cases} \tag{2}$$

Where:

h_i : Handling time at the TAZ *i*.

To account for the temporal effects using link volumes, a binary variable δ_{am}^k indicates if tour *m* reaches TAZ *i* during the interval *k*:

$$\delta_{am}^k = \begin{cases} 1, \; if \;\; (k-1)\Delta \le (d-1)*\Delta + \eta_m^i(d) + h_i < k\Delta \\ \quad 0, \; otherwise \end{cases} \tag{3}$$

Where:

τ_a : Travel time of link *a*.

2.2. Notation

Sets

K : Number of time intervals;
M : Total number of possible tours in the system;
N : Total number of nodes in the system;
W : System entropy that represents the number of ways of distributing freigh vehicle tour flows;
X : Total number of freight vehicle tour flows in the network.

Variables

x_m^d : Tour flow following tour structure *m* starting at time interval *d*;
d : Time interval of tour *m*'s start time;
k : Time interval when tour *m* arrives to the tail node of link *a* ;
O_i^k : Trip production of zone i during time interval k;
D_i^k : Trip attraction of zone i during time interval k;
g_{im}^k : Binary variable equal to 1 if tour m reaches zone i during time interval k, otherwise zero;
γ_{im}^k : Binary variable equal to 1 if tour m leaves zone i during time interval k, otherwise zero;
δ_{am}^k : Binary variable equal to 1 if tour m reaches link a during interval k, otherwise zero;
λ_i^k : Lagrange multiplier associated with the zone i's trips attraction at time k constraint;
β : Lagrange multiplier associated with total impedance constraint;
x_{ij} : Number of vehicles traveling from zone i to zone j;
ψ^k_{ijm} : A binary variable equal to 1 if OD pair ij is in tour *m* during interval k, otherwise 0;
$C_X^{x_m^d}$: Combination of selecting the number of tour flow x_m^d from X;
e(x) : Total squared error between traffic volumes estimates and traffic counts;
ε : Aspiration level of the error of traffic volumes estimates in the ε –constraint method.

Parameters

C : Total impedance in the network;
c_m : Impedance of tour *m;*
α_i^k : Lagrange multiplier associated with zone i's trips production at time k constraint;
ρ : Parameter to create experimental flows;
$\bar{p}_m^{ka}$: The proportion of trips of tour *m* ϵ M at time interval *k* traversing link a ϵ A;

2.3. Mathematical Formulations

Two formulations are proposed for the main component, the first one is the time-dependent entropy maximization (TD-EM) problem that takes advantage of TD freight trip generation, while the second one is a time-dependent ODS (TD-ODS) that incorporates TD traffic counts to reproduce flows.

More specifically, the TD-EM formulation obtains the most likely meso states (i.e., TD tour flows) comprised of micro states (i.e., TD freight vehicle journeys), that are consistent with a set of macro states (i.e., TD trip productions/trip attractions and total tour impedance), as shown in Program TD-EM.

PROGRAM TD-EM

$$\text{Maximize } W = C_X^{x_1} \bullet C_{(X-x_1)}^{x_2} = \frac{X!}{\prod_{m,d}^{M,K'} x_m^d!} \tag{4}$$

Subject to:

$$\sum_{d=1}^{K'} \sum_{m=1}^{M} g_{im}^k x_m^d = O_i^k, \quad \forall i \in \{1,2,...,N\}, \forall k \in \{1,2,...,K\} \quad (\alpha_i^k) \tag{5}$$

$$\sum_{d=1}^{K'} \sum_{m=1}^{M} \gamma_{im}^k x_m^d = D_i^k, \quad \forall i \in \{1,2,...,N\}, \forall k \in \{1,2,...,K\} \quad (\lambda_i^k) \tag{6}$$

$$\sum_{d=1}^{K'} \sum_{m=1}^{M} c_m x_m^d = C \qquad (\beta) \tag{7}$$

$$x_m^d \geq 0, \qquad \forall m \in \{1,2...,M\}, d \in \{1,2...,K\} \tag{8}$$

The TD-ODS is a bi-objective optimization problem, in which the first objective is an entropy maximization (EM) formulation that finds the most likely flow distribution satisfying a set of constraints (i.e., demand and total impedance of the network); while the second objective minimizes the square differences between observed and estimated link flows, as shown in Program TD-ODS. The resulting Pareto frontier reveals the tradeoffs between EM and minimizing traffic estimation's error.

PROGRAM TD-ODS

$$\text{Minimize } z(x) = \sum_{d=1}^{K} \sum_{m=1}^{M} \left(x_m^d \ln(x_m^d) - x_m^d \right) \tag{9}$$

$$\text{Minimize } e(x) = \sum_{a=1}^{A} \sum_{k=1}^{K} \frac{1}{2} \left(v_a^k - \sum_{d=1}^{K'} \sum_{m=1}^{M} \bar{p}_m^{ka} \delta_{am}^{kd} x_m^d \right)^2 \tag{10}$$

Subject to:

$$\sum_{d=1}^{K} \sum_{m=1}^{M} g_{im} x_m^d = O_i \qquad \forall i \in N \tag{11}$$

$$\sum_{d=1}^{K} \sum_{m=1}^{M} \gamma_{jm} x_m^d = D_j \qquad \forall j \in N \tag{12}$$

$$\sum_{d=1}^{K} \sum_{m=1}^{M} c_m x_m^d = C \tag{13}$$

$$x_m^d \geq 0, \qquad \forall m \in M, d \in K \tag{14}$$

3. EXPERIMENTAL SETUP

The effectiveness of the models is assessed using a test case. For the TD-EM model, the inputs are the demand in truck trips for each time interval and TAZ, the link-node incidence matrix characterizing the network, and the sample set of feasible tour sequences. The expected output are the flows for the various tours, which are also defined by their starting times. For the TD-ODS, the inputs also include traffic volumes for each time interval and link, and trips destinations are provided in daily terms.

The experiment uses an artificial network with hypothetical flows that were created by the author. The test values are referred to in this paper as “experimental,” while the estimates produced by the models are termed “estimated.” Figure 2 shows the test case with five TAZ where the nodes represent the centroids. Although in reality the zones would be connected by a set of directional links, for simplicity, the TAZs are assumed to be connected by super-links that represent the shortest path—or any other suitable measure of network impedance—between the centroids. In the figureFigure 2, the travel time (*t*) between zones is indicated on the edges, and the handling time (*h*) is indicated on the centroids.

The tour sequences (twelve different sequences for each starting time) and the tour flows are designed to have significant overlap, so that each TAZ is visited by a number of different tours. To simulate real conditions, the tour impedance cannot exceed twelve hours. The day is discretized into three time intervals. The experimental flows were created using an exponential impedance function, so that the flow decreases with the impedance of the tour to reproduce the tour patterns found in (Holguín-Veras and Thorson, 2000; Wang and Holguín-Veras, 2009). The flows can therefore be expressed as follows:

$$x_m = \rho \exp(U_m) = \rho \exp(-\beta c_m) \qquad \forall m \in M \tag{15}$$

As shown, the deterrence function depends on the disutility U_m, which is the product of a friction factor and the impedance of tour *m*. Taking the derivative of the disutility function with respect to c_m , one finds that the parameter is the marginal disutility of travel:

$$\frac{\partial U_m}{\partial c_m} = \frac{\partial(\beta c_m)}{\partial c_m} = -\beta \qquad \forall m \in M \tag{16}$$

The results show that the parameter of the entropy model is related to the flow patterns. In fact, in the case of the gravity model that uses a simple OD matrix, the average of the inverse of the OD impedances is used as an estimator of the parameter of the gravity model (Ortúzar and Willumsen, 2001). Based on this result, the authors assumed that the parameter of the tour flow model could be approximated by the equal to the inverse of the average tour impedance (7.22 hours), which leads to $\beta_{tour}^{average}$=0.138.

To split the (daily) experimental flows among different time intervals the authors assumed that the temporal split of the flows were 45%, 35%, and 20%, for the first, second, and third interval, respectively. The tour sequences and flows are depicted in Figure 3.

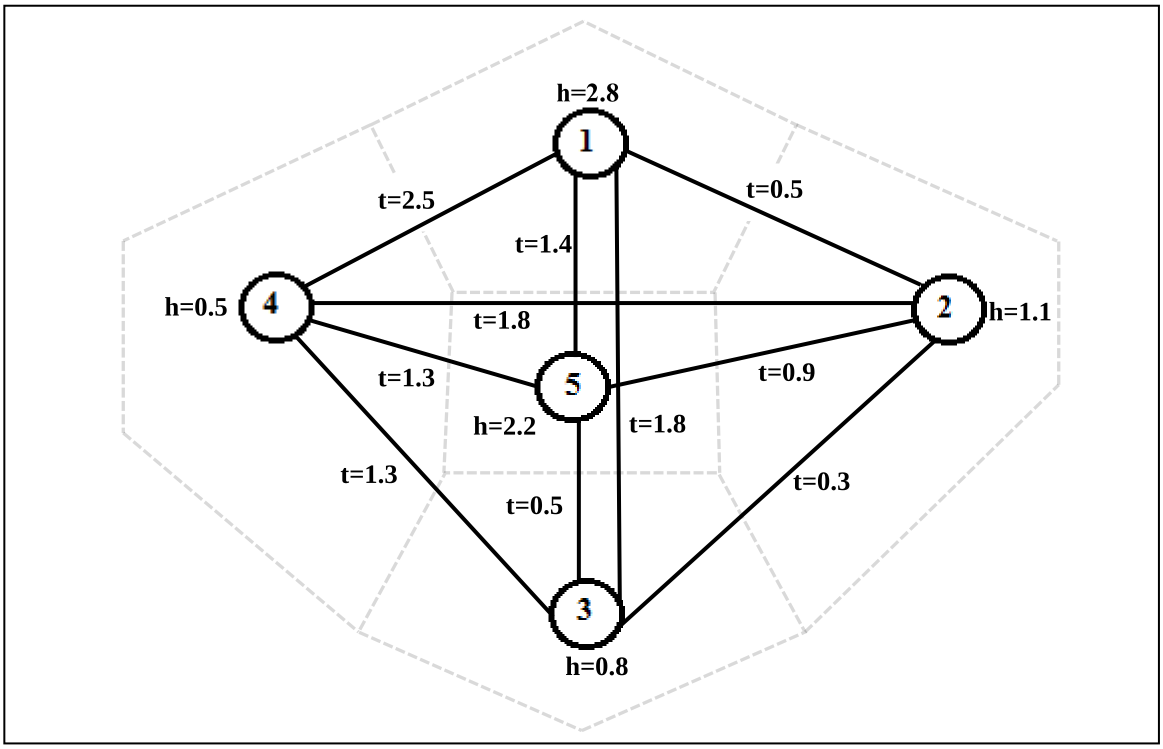

Figure 2: Artificial Network with Travel and Handling Impedances (in Hours)

As shown, every tour sequence has a different flow ranging from 216 to 545 trucks, while total tour impedance ranges from 4.4 hours to 11.1 hours. Some non-optimal tours (i.e., tours 7 and 9) are included to represent the more general scenario in which market constraints, such as delivery time windows, might affect the optimality of the actual routing.

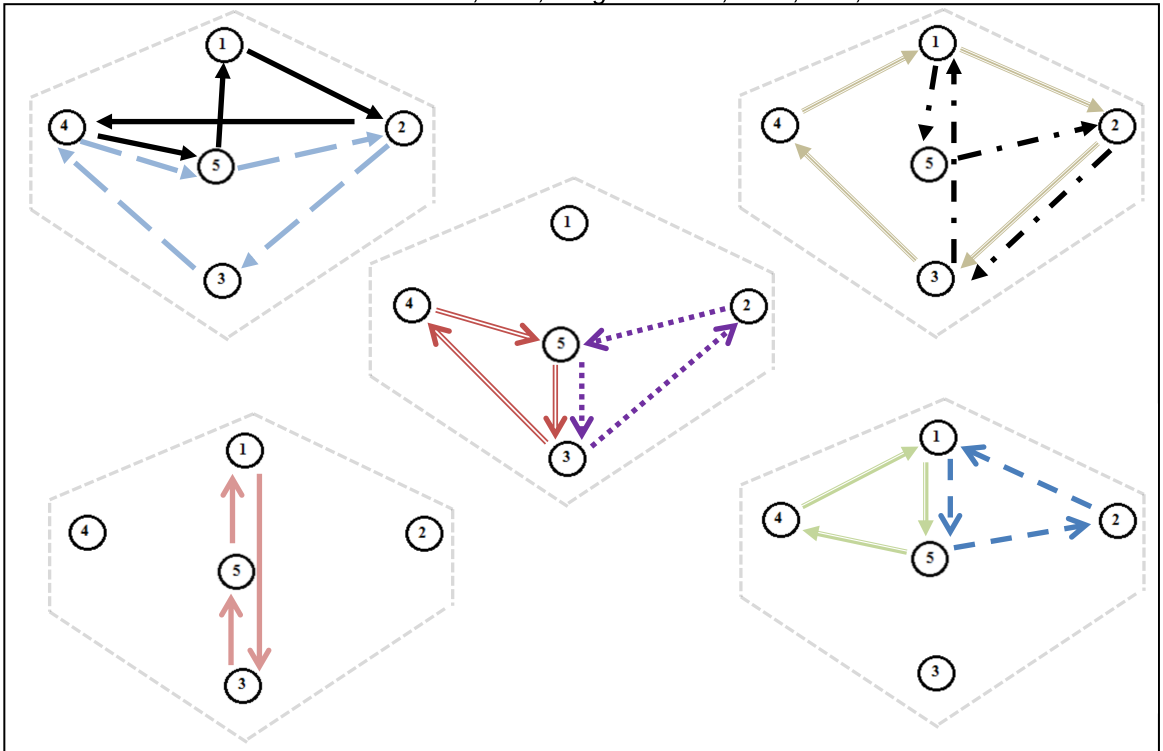

Tour Number	Tour Structure	Tour Daily Trucks Flow	Tour Flow
1	1-2-3-4-1	381	
2	1-5-4-1	336	
8	4-5-1-4	245	
3	2-3-4-5-2	365	
5	4-5-2-3-4	336	
4	2-1-5-2	341	
6	4-5-3-4	431	
10	5-4-3-5	545	
7	4-5-1-2-4	216	
9	5-2-3-1-5	285	
11	3-2-5-3	502	
12	3-5-1-3	301	

Figure 3: Tours Sequences and Flows

Using the tour flows and the binary variables g_{im}^{k} and γ_{im}^{k}, the trip productions and attractions for each zone and time interval are generated. However, since the time intervals are relatively long, some tour flows arrive and leave the TAZs in the same time interval; therefore it is necessary to drop some trip production constraints to avoid the degeneracy caused by redundant constraints. In contrast, in the S-EM and the TD-ODS cases, attractions and productions are equal, so only one set of constraints is used. The productions and attractions resulting from the experimental setting are shown in Table 1. The TD productions and attractions are used as inputs for the TD-EM, and the static attractions by the S-EM and the

TD-ODS. Computing the TD trip productions and attractions is crucial because they are one of the factors that determine the time-dependent nature of the TD-EM problem.

Table 1: Experimental Trip Generation Values

	Experimental TD-Productions			Experimental TD-Attractions			Experimental S-Productions/ S-Attractions (daily)
TAZ	K=1	K=2	K=3	K=1	K=2	K=3	
1	945	737	423	945	737	423	2105
2	993	871	519	993	871	519	2426*
3	1414	1102	630	1279	1132	674	3146*
4	1283	1001	571	1076	1046	641	2855*
5	1754	1368	781	1626	1396	824	3903*

Notes: (*) These values do not match the summation of the TD-EM inputs because some tours starting in K=3 do not finish the tour in the same day

Similarly, Table 2 presents the TD traffic counts used for inputs in the TD-ODS model.

Table 2: Experimental Time-Dependent Traffic Counts

Superlink	**Traffic Counts-Time Interval**		
	K=1	**K=2**	**K=3**
1 - 2	171	230	153
1 - 3	0	135	105
1 - 4	0	110	86
1 - 5	304	365	236
2 - 1	153	119	69
2 - 3	614	479	274
2 - 4	0	97	76
2 - 5	226	176	100
3 - 1	128	100	57
3 - 2	226	176	100
3 - 4	680	530	303
3 - 5	380	296	170
4 - 1	322	251	144
4 - 3	245	191	109
4 - 5	716	559	318
5 - 1	342	267	153
5 - 2	596	465	266
5 - 3	420	327	186
5 - 4	396	309	176

4. RESULTS

4.1. TD-EM

After setting up the experimental case, both the S-EM (Wang and Holguín-Veras, 2009) and the TD-EM models were calibrated using minos solver in AMPL. The S-EM took 0.012

seconds to complete the computations, while the TD-EM took 0.078 seconds. Table 3 shows the observed and estimated flows using the S-EM and the TD-EM models.

Table 3: Tour Flow Estimates

Tour Sequence	TAZs visited	Tour Impedance (in hours)	Experimental Flows				Estimated Flows				
							S-EM	TD-EM			
			Daily	d=1	d=2	d=3	Daily	d=1	d=2	d=3	Daily
1	1 - 2 - 3 - 4	7.0	381	171	133	77	217	171.0	133.0	77.0	381.0
2	1 - 5 - 4 - 0	7.9	336	151	118	67	399	150.9	117.8	67.4	336.0
3	2 - 3 - 4 - 5	7.3	365	164	128	73	523	164.0	128.1	72.9	365.0
4	2 - 1 - 5 - 0	7.8	341	153	119	69	160	153.1	119.2	68.6	341.0
5	4 - 5 - 2 - 3	7.9	336	151	118	67	390	151.0	117.9	67.1	336.0
6	4 - 5 - 3 - 0	6.1	431	194	151	86	279	193.9	151.2	85.9	431.0
7	4 - 5 - 1 - 2	11.1	216	97	76	43	282	97.1	76.0	43.1	216.2
8	4 - 5 - 1 - 0	10.2	245	110	86	49	130	109.9	86.0	48.9	244.8
9	5 - 2 - 3 - 1	9.1	285	128	100	57	676	128.0	100.0	57.0	285.0
10	5 - 4 - 3 - 0	4.4	545	245	191	109	638	245.2	191.1	108.7	545.0
11	3 - 2 - 5 - 0	5.0	502	226	176	100	182	225.9	175.8	100.4	502.0
12	3 - 5 - 1 - 0	8.7	301	135	105	61	244	135.0	105.0	61.0	301.0
Root Mean Squared Error (RMSE)							178.89	0.17			

The tour flows estimated using TD-EM match very closely the experimental flows. Although the S-EM does provide fairly good estimates, the root mean square error (RMSE) clearly indicates that the TD-EM model does a better job in replicating the experimental values (0.17 versus 178.89). This is a result of the incorporation of time-dependent effects, which not only provides additional constraints related to time; but also enables to differentiate between production and attraction constraints. While the S-EM requires flow conservation over the period of study (total productions=total attractions), the TD-EM allows tours to start in one interval and finish in another one. In terms of time-dependency, the flows estimated by the TD-EM match the input values (45%, 35%, and 20%), which shows that the model captures the temporal aspects of tour flows.

The Lagrange multipliers associated with the various constraints are interesting outputs. Table 4 shows the Lagrange multipliers for both the static and the time-dependent scenario. For the time-dependent scenario, each TAZ has trips attractions Lagrange multiplier (α_i^k) for each time interval, trips productions Lagrange multiplier (λ_i^k) for time intervals and TAZs where productions differ from attractions, and for the total impedance (β).

Table 4: Lagrange Multipliers for Trip Attraction Constraints

Lagrange Multipliers associated to TAZ by Time Interval								
TD-EM Model								**S-EM Model**
TD Attractions				**TD Productions**				
L.Mult.	**k=1**	**k=2**	**k=3**	**L.Mult.**	**k=1**	**k=2**	**k=3**	**Day**
α_1^k	3.055	2.927	2.659	λ_1^k	n/a	n/a	n/a	3.358
α_2^k	-0.002	0.000	0.001	λ_2^k	n/a	n/a	n/a	1.233
α_3^k	8.638	5.577	2.645	λ_3^k	-5.581	-2.649	0.008	2.103
α_4^k	0.000	0.001	0.004	λ_4^k	-0.003	0.000	-0.007	2.198
α_5^k	8.641	5.584	2.659	λ_5^k	-5.586	-2.653	-0.014	4.411
Lagrange Multipliers associated to total impedance								
β	-0.138							-0.498

As shown, the values of α_i^k range from -0.002 to 3.055 for the time-dependent case, and from 1.212 to 4.350 for the static case. In the case of $\lambda_i{}^k$, TAZs 1 and 2 do not have an associated production Lagrange multiplier because tours enter and leave the TAZs in the same time interval. The other TAZs have associated multipliers ranging from -5.581 to 0.008. The Lagrange multiplier associated with the tours impedance (β^*) is negative in both the TD-EM and the S-EM models. For the TD-EM this value is very close to the one use to create the experimental flows ($\beta_{tour}^{average} = 0.138$).

The tour experimental and estimated flows are converted to OD matrices. TD-EM flows are assigned to time intervals based on their arrival time; therefore, the totals for daily productions match the experimental productions presented in Table 1 but not necessarily the daily attractions. The resulting OD matrices are shown in Table 5. The results show the daily OD matrices estimated by both models both for daily totals, and time of day. In the case of the S-EM, the time-dependent matrices were estimated in proportion to the time of day split (45%, 35%, and 20%); while for the TD-EM model, the matrices are a direct output of the model. The table also shows the correlation coefficients, mean absolute percentage errors (MAPEs) and RMSEs for the different matrices.

Table 5: Daily and Time-Dependent Origin-Destination Matrices

Daily

Experimental Flows

O\D	1	2	3	4	5	Total
1	0	554	240	196	905	1895
2	341	0	1367	173	502	2383
3	285	502	0	1513	846	3146
4	717	0	545	0	1593	2855
5	762	1327	933	881	0	3903
Total	2105	2383	3085	2763	3846	14182

Estimated S-EM Flows

O\D	1	2	3	4	5	Total
1	0	496	244	130	1235	2105
2	160	0	1803	282	182	2427
3	676	182	0	1406	882	3146
4	613	0	638	0	1604	2855
5	656	1749	461	1037	0	3903
Total	2105	2427	3146	2855	3903	14436

Correlation: 0.90; MAPE: 34.6%

Estimated TD-EM Flows

O\D	1	2	3	4	5	Total
1	0	554	240	196	905	1895
2	341	0	1367	173	502	2383
3	285	502	0	1513	846	3146
4	717	0	545	0	1593	2855
5	762	1327	933	881	0	3903
Total	2105	2383	3085	2763	3846	14182

Correlation: 1.00; RMSE: 0.06

K=1

Experimental Flows

O\D	1	2	3	4	5	Total
1	0	171	0	0	304	475
2	153	0	614	0	226	993
3	128	226	0	680	380	1414
4	322	0	245	0	716	1283
5	342	596	420	396	0	1754
Total	945	993	1279	1076	1626	

Estimated S-EM Flows

O\D	1	2	3	4	5	Total
1	0	223	110	59	556	947
2	72	0	811	127	82	1092
3	304	82	0	633	397	1416
4	276	0	287	0	722	1285
5	295	787	207	467	0	1756
Total	947	1092	1416	1285	1756	

Correlation: 0.87; MAPE: 53.7%

Estimated TD-EM Flows

O\D	1	2	3	4	5	Total
1	0	171	0	0	304	475
2	153	0	614	0	226	993
3	128	226	0	680	380	1414
4	322	0	245	0	716	1283
5	342	596	420	396	0	1754
Total	945	993	1279	1076	1626	

Correlation: 1.00; RMSE: 0.10

K=2

Experimental Flows

O\D	1	2	3	4	5	Total
1	0	230	135	110	365	840
2	119	0	479	97	176	871
3	100	176	0	530	296	1102
4	251	0	191	0	559	1001
5	267	465	327	309	0	1368
Total	737	871	1132	1046	1396	

Estimated S-EM Flows

O\D	1	2	3	4	5	Total
1	0	174	85	46	432	737
2	56	0	631	99	64	849
3	237	64	0	492	309	1101
4	215	0	223	0	561	999
5	230	612	161	363	0	1366
Total	737	849	1101	999	1366	

Correlation: 0.91; MAPE: 49.1%

Estimated TD-EM Flows

O\D	1	2	3	4	5	Total
1	0	230	135	110	365	840
2	119	0	479	97	176	871
3	100	176	0	530	296	1102
4	251	0	191	0	559	1001
5	267	465	327	309	0	1368
Total	737	871	1132	1046	1396	

Correlation: 1.00; RMSE: 0.14

K=3

Experimental Flows

O\D	1	2	3	4	5	Total
1	0	153	105	86	236	580
2	69	0	274	76	100	519
3	57	100	0	303	170	630
4	144	0	109	0	318	571
5	153	266	186	176	0	781
Total	423	519	674	641	824	

Estimated S-EM Flows

O\D	1	2	3	4	5	Total
1	0	99	49	26	247	421
2	32	0	361	56	36	485
3	135	36	0	281	176	629
4	123	0	128	0	321	571
5	131	350	92	207	0	781
Total	421	485	629	571	781	

Correlation: 0.90; MAPE: 81.7%

Estimated TD-EM Flows

O\D	1	2	3	4	5	Total
1	0	153	105	86	236	580
2	69	0	274	76	100	519
3	57	100	0	303	170	630
4	144	0	109	0	318	571
5	153	266	186	176	0	781
Total	423	519	674	641	824	

Correlation: 1.00; RMSE: 0.24

Table 5 shows that, in general, the TD-EM does an excellent job in replicating the experimental OD matrix. TD-EM estimates are basically the same than the experimental flows for each time interval. The S-EM estimates present slight differences in daily estimates with a MAPE of 34.6% and a fairly high correlation (0.90) between the modeled and the experimental values. However, the S-EM MAPE is much higher for the time dependent matrices; for instance, the third interval shows an 81.7% error. This confirms the TD-EM model's ability to reproduce the underlying flow patterns quite well; but also the potential errors of using a naïve approach to distribute S-EM flows between time intervals.

Figure 4 shows for both experimental and estimated daily values, the OD flows as a function of OD impedances; while Figure 5 shows the tour flows as a function of tour impedances. To provide an indication of the degree of statistical association between flows and impedances, the correlation of coefficients are also shown. The most obvious feature of Figure 4 is that the lack of a discernible pattern that could hint at linkage between OD flows and OD impedances. Moreover, since the correlation coefficients are positive—which is conceptually incorrect—the inescapable conclusion is that the relation between OD flows and OD impedances is shaky to say the least.

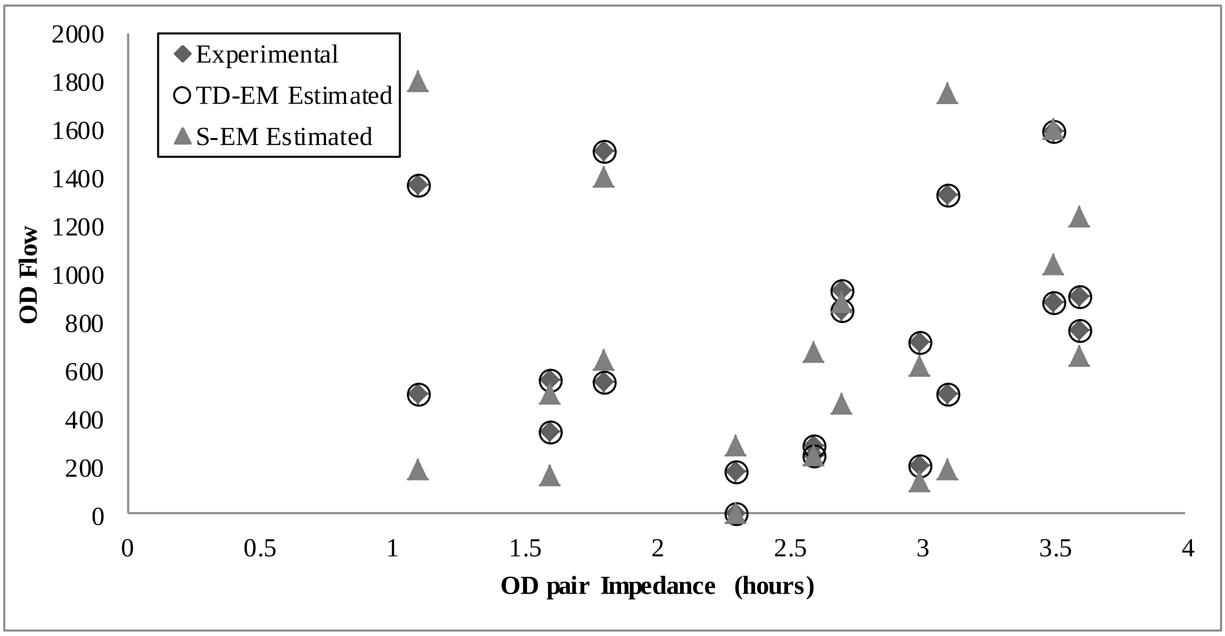

Figure 4: OD Flows versus OD Impedances

Note: Correlation (Experimental, OD Impedance)=0.13; Correlation(TD-EM, OD Impedance)=0.13; Correlation(S-EM, OD Impedance)=0.15.

Figure 5 shows the existence of a clear relation between tour flows and tour impedances which also depends on the model used to produce the estimates. In the case of the S-EM model, the results show a negative relation between flows and impedances, as expected, though the degree of statistical association (-0.20) was relatively low. In contrast, the TD-EM model accurately replicates the experimental values leading to a high correlation between flows and impedances. In essence, the quality of the model influences the quality of the results.

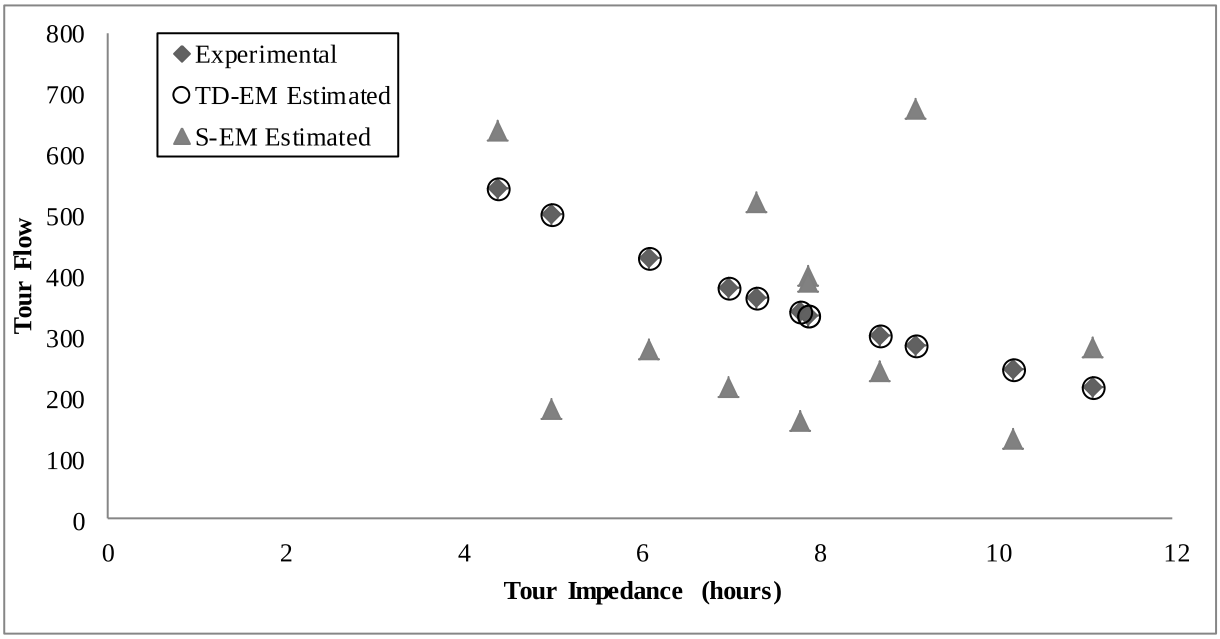

Figure 5: Tour Flows versus Tour Impedances

Note: Correlation(Experimental, Tour Impedance)=-0.98; Correlation(TD-EM, Tour Impedance)=-0.98; Correlation(S-EM, Tour Impedance)=-0.20.

4.2. TD-ODS

As explained in the formulation of TD-ODS 1, the model is comprised by two objective functions: the EM and the function to replicate traffic volumes. Using the ε-constraint method, it is possible to generate a Paretto efficient frontier representing the tradeoffs between the two conflicting objectives as shown in Figure 6.

The figure reveals the conflicting nature of these two objectives: an increase in the aspiration level (ε) for the traffic replication objective function produces a decrease in the entropy objective function. This relationship can be approximated by a polynomial function with a high R^2 (0.987). Therefore, the unitary change depends on the aspiration level according to the following expression:

$$\frac{\partial\left(0.0025\varepsilon^2 - 0.5331\varepsilon + 16556\right)}{\partial\varepsilon} = 0.005\varepsilon - 0.5331 \qquad (17)$$

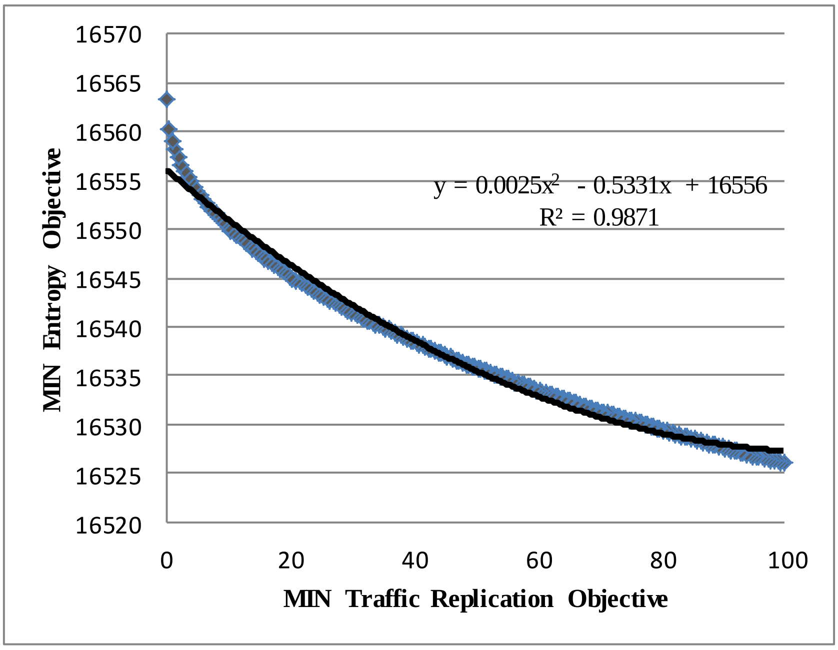

Figure 6: Paretto Efficient Frontier

Tour flows are then estimated for every aspiration level and the performance of the model to reproduce tour flows is assessed through a RMSE analysis. The model is implemented using the minos solver in ampl; the time required to solve the problem ranges from 0.60 seconds for ε=100 to 2.74 seconds for ε=0.5. Table 6 presents the results for three aspiration levels (ε =0.25, ε =25 and ε =50).

Table 6: Tour Flow Estimates for the TD-ODS 2

Tour Sequence	TAZs visited	Tour Impedance (in hours)	Experimental Flows			Estimated Flows								
						TD-ODS: ε =50			TD-ODS: ε =25			TD-ODS: ε =0.25		
			d=1	d=2	d=3	d=1	d=2	d=3	d=1	d=2	d=3	d=1	d=2	d=3
1	1-2-3-4	7.0	171	133	77	168.6	130.5	75.3	169.3	131.2	75.7	170.8	132.8	76.8
2	1-5-4-0	7.9	151	118	67	153.5	120.2	69.5	152.8	119.6	68.9	151.2	118.2	67.2
3	2-3-4-5	7.3	164	128	73	170.8	133.8	75.5	169.0	132.2	74.8	164.5	128.5	73.1
4	2-1-5-0	7.8	153	119	69	148.8	114.4	65.4	150.0	115.7	66.3	152.7	118.7	68.7
5	4-5-2-3	7.9	151	118	67	145.0	113.6	64.1	146.5	114.7	64.9	150.5	117.6	66.9
6	4-5-3-0	6.1	194	151	86	194.4	151.4	87.9	194.5	151.4	87.5	194.1	151.1	86.2
7	4-5-1-2	11.1	97	76	43	98.5	77.3	55.4	97.9	76.8	53.0	97.0	76.0	44.3
8	4-5-1-0	10.2	110	86	49	107.5	83.9	36.9	108.4	84.7	38.9	109.9	85.9	47.6
9	5-2-3-1	9.1	128	100	57	130.6	102.4	61.6	129.8	101.7	60.1	128.2	100.2	57.3
10	5-4-3-0	4.4	245	191	109	243.3	189.8	108.4	243.7	190.1	108.4	244.9	190.9	108.9
11	3-2-5-0	5.0	226	176	100	222.9	173.4	98.1	223.7	174.1	98.5	225.8	175.8	99.8
12	3-5-1-0	8.7	135	105	61	135.7	105.9	63.1	135.6	105.7	62.8	135.1	105.1	61.3
Root Mean Squared Error (RMSE)						4.14			3.20			0.40		

As expected, the smaller the aspiration level and the better the model performs. For instance, the RMSE for ε=50 is about 10 times higher than the one for 0.25. The error for ε=50 (RMSE=4.14) is larger than the one found for the TD-EM model (RMSE=0.17); though substantially lower than the one obtained from the S-EM (RMSE 178.89). In essence, the TD-ODS model represents a great enhancement for tour-based modeling because it reproduces very closely time-dependent tour flows without the costly data requirements from the traditional approach, and what is more, without requiring TD freight trip generation as in the case of TD-EM.

Another interesting output from the model are the Lagrangian multipliers for each constraint, including the ε-constraint. As shown in Table 7, the values for the multipliers vary according to the aspiration level, though the sign remains the same. The multipliers associated with the destinations constraint are always positive and range from 0.062 to 2.873. In contrast, the multiplier for the traffic constraint (i.e., the ε-constraint) is always negative and decreases with the value of ε; it ranges from -3.055 to -0.164. In the case of the cost multiplier, the value ranges from -0.272 to -0.140, and tends to the experimental β (-0.138) when ε tends to 0.

Table 7: Lagrange Multipliers for TD-ODS Constraints

TD-ODS Model				
Lagrange Multipliers		**ε-constraint value**		
		ε=50	**ε=25**	**ε=0.25**
Destinations	λ_1	2.495	2.380	2.108
	λ_2	0.653	0.522	0.062
	λ_3	1.798	1.787	1.765
	λ_4	1.689	1.656	1.580
	λ_5	2.873	2.753	2.467
Cost	β	-0.272	-0.237	-0.140
Traffic	χ	-0.164	-0.246	-3.055

5. CONCLUSIONS

The assessment of the TD-EM and the TD-ODS reveals the great potential of these models to capture the temporal aspects from variations in freight trip generation and traffic volumes respectively. The enhanced freight trip distribution models proposed provide a substantial contribution to transportation modeling, as they reproduce the TD tour-based behavior inherent to freight vehicles and is bound to improve significantly the precision of urban transportation plans.
Some fundamentals findings from this research are summarized as follows:

1. Wang and Holguín-Veras (2009) and (Holguín-Veras and Thorson, 2000) show that there is not a clear linkage between OD flows and OD impedances for freight where tour impedances are key to explain flows. This paper shows that a trip-based model does not reproduce this pattern. Therefore, freight demand models must consider tour-based behavior.

2. TD-EM model has the best performance by far but requires time-dependent freight trip generation information, which is difficult to obtain. In the cases where data availability is not a problem this model has a great potential. However, in most cases time-dependency of freight trip generation is obtained from traffic counts; thus implementing a TD-ODS will deliver more accurate and reliable estimates.

3. Both calibration information and time-dependency can be obtained in a cost-efficient way from traffic counts, with an encouraging precision (depending on the aspiration level set by the modeler).

4. Some considerations to design the aspiration level of the TD-ODS include the confidence that the traffic assignment algorithm implemented replicates freight-vehicles behavior and the level of confidence on the traffic counts.

REFERENCES

Boerkamps, J. and A. van Binsbergen (1999). Goodtrip - A New Approach for Modelling and Evaluation of Urban Goods Distribution. City Logistics I, Cairns, Australia.

Donnelly, R. (2007). A hybrid microsimulation model of freight flows. Proceedings of the 4th International Conference on City Logistics, July 11-13, 2007. E. Taniguchi and R. G. Thompson. Crete, Greece, Institute for City Logistics**:** 235-246.

Donnelly, R. (2010). Best Practices for Incorporating Commodity Flow Survey and Related Data Into the MPO and Statewide Planning Processes. **NCHRP Project 08-36.**

Holguín-Veras, J. (2000). A Framework for an Integrative Freight Market Simulation. IEEE 3rd Annual Intelligent Transportation Systems Conference ITSC-2000, Dearborn Michigan, IEEE

Holguín-Veras, J. and E. Thorson (2000). "An Investigation of the Relationships between the Trip Length Distributions in Commodity-based and Trip-based Freight Demand Modeling." Transportation Research Record **1707**: 37-48.

Holguín-Veras, J., N. Xu and J. Mitchell (2012). "A Dynamic Spatial Price Equilibrium Model of Integrated Production-Transportation Operations Considering Freight Tours." (in review).

Holguín Veras, J., E. Thorson, Q. Wang, N. Xu, C. González, I. Sánchez-Díaz and J. Mitchell (2012). Urban Freight Tour Models: State of The Art And Practice. i. review).

Hunt, J. D. and K. J. Stefan (2007). "Tour-based microsimulation of urban commercial movements." Transportation Research Part B: Methodological **41**(9): 981-1013.

Liedtke, G. (2006). An actor-based approach to commodity transport modelling. Baden-Baden, Nomos, Karlsruhe Universität. **Ph.D.**

Liedtke, G. (2009). "Principles of micro-behavior commodity transport modeling." Transportation Research Part E: Logistics and Transportation Review **45**(5): 795-809. 10.1016/j.tre.2008.07.002

Liedtke, G. and H. Schepperle (2004). "Segmentation of the transportation market with regard to activity-based freight transport modelling." International Journal of Logistics Research and Applications: A Leading Journal of Supply Chain Management **7**(3): 199 - 218.

Meyer, M. D. and E. J. Miller (1984). Urban transportation planning: A decision-oriented approach, McGraw-Hill (New York)

Ogden, K. W. (1978). "The distribution of truck trips and commodity flow in urban areas: A gravity model analysis." Transportation Research **12**(2): 131-137.

Ortúzar, J. D. and L. G. Willumsen (2001). Modelling Transport. New York, John Wiley and Sons.

Routhier, J. L. and F. Toilier (2007). FRETURB V3, a policy oriented software tool for modelling urban goods movement. 11th World Conference on Transport Research, Berkeley, CA.

Stefan, K., J. McMillan and J. Hunt (2005). "Urban Commercial Vehicle Movement Model for Calgary, Alberta, Canada." Transportation Research Record: Journal of the Transportation Research Board **1921**: 1-10.
Taniguchi, E. and R. G. Thompson (2002). "Modeling city logistics." Transportation Research Record **1790**: 45-51.
Thorson, E. (2005). The Integrative Freight Market Simulation: An Application of Experimental Economics and Algorithmic Solutions. Civil and Environmental Engineering. Troy, NY, Rensselaer Polytechnic Institute. **Ph.D.:** 156.
van Duin, J. H. R., L. A. Tavasszy and E. Taniguchi (2007). "Real time simulation of auctioning and re-scheduling processes in hybrid freight markets." Transportation Research Part B: Methodological **41**(9): 1050-1066. 10.1016/j.trb.2007.04.007
Wang, Q. and J. Holguín-Veras (2008). "Investigation of Attributes Determining Trip Chaining Behavior in Hybrid Microsimulation Urban Freight Models." Transportation Research Record: Journal of the Transportation Research Board **2066**: 1-8.
Wang, Q. and J. Holguín-Veras (2009). Tour-based Entropy Maximization Formulations of Urban Commercial Vehicle Movements. 2009 Annual Meeting of the Transportation Research Board. **CDROM**.
Wisetjindawat, W., K. Sano, S. Matsumoto and P. Raothanachonkun (2007). Micro-Simulation Model for Modeling Freight Agents Interactions in Urban Freight Movement. 86th Annual Meeting of the Transportation Research Board
Xu, N. and J. Holguín-Veras (2008). A Dynamic Model of Integrated Production-Transportation Operations. Annual Meeting of the Transportation Research Record.